 

PACS numbers: 42.55.Lt; 42.60.Gd; 52.50.Jm
DOI: 10.1070/QE2014v044n01ABEH015265

# Influence of an optical pulsed discharge on the structure of a supersonic air flow

A.N. Malov, A.M. Orishich

*Abstract.* **We present the results of investigation of the parameters of an optical pulsed discharge (OPD) and their relation with gas-dynamic parameters of a supersonic flow and with characteristics of laser radiation. For the first time the discrete objects are detected in the OPD by an optical method, namely, low-density caverns moving along with the flow. The propagation velocity of the thermal track arising in a supersonic flow under the action of the OPD is measured. It is found that at a pulse repetition rate of 90–120 kHz the caverns unite into a single plasma jet.**

***Keywords:*** *high-power repetitively pulsed $CO_2$ laser, mechanical Q-switching, supersonic air flow, optical pulsed discharge, air optical breakdown, thermal track, low-density cavern.*

## 1. Introduction

Employment of laser radiation for obtaining an optical discharge in a supersonic air flow and for developing methods for efficient energy absorption in it is promising in investigations aimed at solving problems of controlling the parameters of aerodynamics of aircrafts, plasma chemistry, burning and so on [1–4]. The optical pulsed discharge (OPD) obtained in [5–8] was ignited in a focus of the radiation pulse of a repetitively pulsed $CO_2$ laser in a supersonic argon flow and affected the flow similarly to a cw optical discharge. But realisation of the OPD in air necessitates a high power of laser radiation. This circumstance stimulated investigations concerning creation of high-power repetitively pulsed lasers. In [9–11] we described a repetitively pulsed $CO_2$ laser with the pulse repetition rate of up to 80 kHz and power of 4.5 kW. The characteristics of the laser made it possible for the first time to obtain the OPD in a supersonic air flow (with the Mach number $M = 2$) and formulate the requirements to gas density and parameters of the radiation pulse, fulfilment of which resulted in obtaining a strong (to 65%) absorption of the radiation power in the flow. The properties of the flow with the OPD and the structure of the gas flow in a thermal track substantially affect the possibilities of controlling aero-dynamic characteristics of a supersonic aircraft, in particular, of elimination of the sonic shock effect [12]. In [10] we obtained the mass-averaged air temperatures along a thermal track after the action of the OPD, which were equal to 120–150 °C. In these experiments we detected a thermal track glow, which cannot be related to the mentioned gas temperature in the flow. Nevertheless, the glow may be related to a glow of caverns arising in the flow in the process of the periodical gas breakdown under the action of laser radiation.

The dynamics of laser spark formation in steady air and hydro-dynamic relaxation of a hot gas cloud have been studied sufficiently well [13–15]. Formation of an actually spherical shock wave was observed as well as relatively slow radial expansion of the glow region of a heated ionised gas or plasma. In recent investigations, problems of laser breakdown at ultrahigh pulse repetition rates are analysed as well as obtaining lengthy plasma channels by a single pulse [16, 17]. In works devoted to spark investigation in steady air [13–15, 18] it was noted that the dynamics of expansion of a plasma ball substantially depends on the conditions of energy supply and may be of complicated asymmetric character. This was explained by peculiarities of gas breakdown, development of a detonation wave along a laser beam, which determines the directional movement of plasma and cold gas, formation of vortex structures and so on. The character of plasma expansion substantially affects its lifetime. The motion dynamics of plasma clouds in the OPD at a high pulse repetition rate ($\sim 10^5$ Hz) and their mutual influence have not been studied previously. Of particular interest is finding the conditions for merging separate plasma clouds to a united plasma jet.

The present work is aimed at obtaining data on spatial, temporal, and spectral characteristics of the optical radiation of the supersonic air flow after it was subjected to an action of the OPD.

## 2. Experimental setup

A repetitively pulsed $CO_2$ laser with mechanical $Q$-switching was used in the experiments. The laser pulse repetition rate was up to 120 kHz and the power was up to 4.5 kW [7–9]. The pulsed power of the laser depending on the modulation conditions was 60–200 kW. The pulse repetition rate of 120 kHz is presently the highest frequency for high-power $CO_2$ lasers with mechanical $Q$-switching. The scheme of the experiments is shown in Fig. 1.

Supersonic flow (*2*) was formed by a conic nozzle (*1*). The conic nozzle with the aperture angle of 13°, diameter of the exit section 10 mm and diameter of the critical cross section 8 mm corresponded to the geometrical Mach number of 1.9. The gas expenditure was 2–4 kg $s^{-1}$. The laser radiation passed through lens (*5*) made of ZnSe with a focal length of 63 mm to the axis line of the supersonic flow perpendicular to

**A.N. Malov, A.M. Orishich** Khristianovich Institute of Theoretical and Applied Mechanics, Siberian Branch, Russian Academy of Sciences, ul. Institutskaya 4/1, 630090 Novosibirsk, Russia;
e-mail: laser@itam.nsc.ru, malex@itam.nsc.ru

Received 24 June 2013; revision received 3 September 2013
*Kvantovaya Elektronika* **44** (1) 83–88 (2014)
Translated by N.A. Raspopov

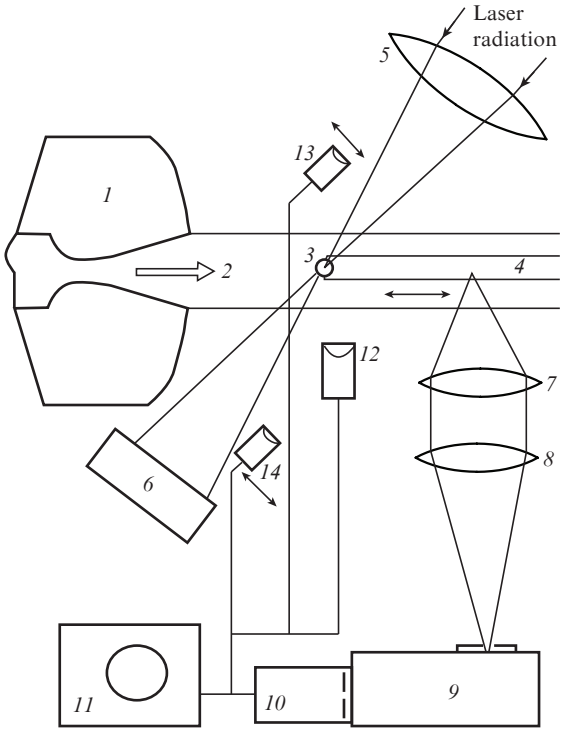


**Figure 1.** Scheme of the experiments: (*1*) conic mirror; (*2*) supersonic flow; (*3*) region of air optical breakdown; (*4*) thermal track; (*5*) lens made of ZnSe; (*6*) calorimetric power meter; (*7*, *8*) lenses of optical tract; (*9*) DMR-4 double monochromator; (*10*) photomultiplier; (*11*) digital oscilloscope; (*12*) coaxial photocell; (*13*, *14*) FD-24K photodiodes.

the direction of gas motion. The spot diameter in the focal plane of the lens was 100–150 μm, which provided the pulsed radiation intensity under optimal operation of $(7-15) \times 10^8$ W cm$^{-2}$ and an optical breakdown in a supersonic air flow (*3*). The laser radiation at the output of the flow and flame zone was measured by a NOVA 2 calorimetric power meter with the limiting measured power of 5 kW (*6*).

An external appearance of the working zone of the installation with an optical discharge in a supersonic air flow is shown in Fig. 2. One can see a spherical glow of optical discharge plasma and a thermal track with the width of ~5 mm and length of ~20-30 mm. For visual observation of the process of plasma formation in a supersonic flow and of the produced thermal track the installation is supplied with an optical diagnostic system. The optical scheme used in this work for measuring a small signal of thermal track radiation against the background of high-power radiation of the plasmoid comprised an optical tract (*7*, *8*) for transferring the image of a point of thermal track (*4*) to an entrance slit of monochromator (*9*). A DMR-4 double monochromator was used, which reliably suppressed extraneous emission. The signal at the output of the monochromator was detected by a FEM-106 photomultiplier (*10*) with the spectral range of sensitivity 170–850 nm and then passed to oscilloscope (*11*). The optical system provided a spatial resolution of ~100 μm for the thermal track, and the electronic detection system had a temporal resolution of ~50 ns. The dynamics of energy absorption in the zone of the optical discharge was measured using FD-24K photodiodes for incident (*13*) and passed (*14*) laser radiation and an FK-22 coaxial vacuum photocell (*12*) for

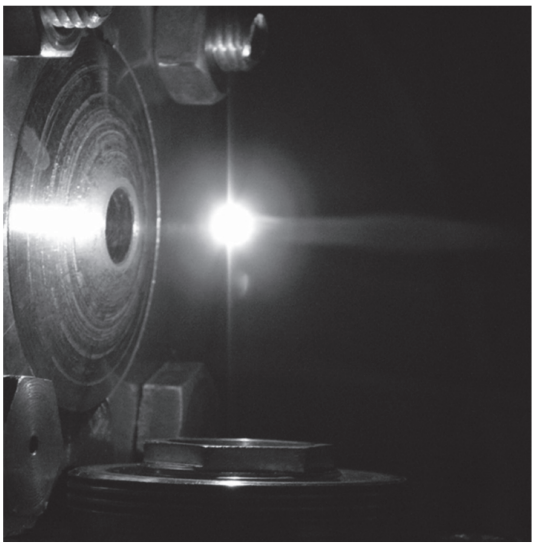

**Figure 2.** Photograph of the operation unit with a burning OPD.

detecting light from the plasmoid. Electrical signals from photodetectors were recorded by oscilloscope (*11*).

## 3. Experimental results

In [11] we thoroughly investigated energy absorption in the process of formation of a separate OPD plasma bunch. After gas breakdown, the ionisation front is generated, which propagates inside the caustic towards the laser beam. At the laser radiation intensities of our experiment ($5 \times 10^8 - 2 \times 10^9$ W cm$^{-2}$), a laser-supported detonation wave may arise [9], which moves at the characteristic velocity of $\sim 2 \times 10^6$ mm s$^{-1}$. The characteristic time of energy absorption was 1 μs and the length of the plasma bunch along the beam at an initial stage of energy absorption was no greater than 1–2 mm, i.e., substantially less than the laser beam diameter (100–150 μm) in the focal plane of the lens. However, intensive side expansion of plasma occurs beyond the front of the laser-supported detonation wave. Thus, a high-pressure bunch of plasma (plasmoid) arises in the laser spark quite rapidly with the shape close to spherical (Fig. 2). In a relatively short time interval, plasma expands radially with a reduction of pressure to the pressure of the ambient medium. In front of expanding plasma, a shock wave arises which is almost spherical. The following relatively slow process of plasma relaxation is isobaric. In the process, the 'quality' of energy deposition determines the degree of plasma turbulisation and, consequently, the rate of its cooling.

Direct measurements in the central high-temperature region of a single discharge were performed in [17] where the temperature dynamics of cylindrical plasma breakdown was studied by spectral methods. It was established that regardless of the value of energy deposition the transition from adiabatic expansion to the isobaric stage occurs at the same temperature ($8500 \pm 500$ K), but at distinct instants. In this case, the initial temperature varies because it depends on the power deposited. The formed hot cloud (cavern) has a very small density. It is important that a cavern glow was observed at both the adiabatic and isobaric stages, i.e., during 300–500 μs. Estimates based on the data from [17, 19] under the conditions of our experiments yield the characteristic time of

completion of adiabatic expansion ~5 μs. Hence, in the course of fast expansion at the velocity of the air flux of ~500 m s$^{-1}$ the cavern covers a distance of 2–3 mm. A further cavern motion in the flow was the subject of our investigation.

In the present work, the spectral characteristics of cavern glow in a supersonic air flow in the OPD have been investigated. The results of intensity measurements of the optical signal at several wavelengths in the range 300–950 nm are shown in Fig. 3. The measurements were taken at the width of monochromator output slit 0.5 mm, which corresponded to the spectral width of passed radiation ~5 nm. In the emission spectrum (Fig. 3), lines of the first $A^3\Sigma_u^+ - B^3\Pi_g$ (460–950 nm) and the second $B^3\Pi_g - C^3\Pi_u$ (300–500 nm) positive bands of nitrogen were reliably detected as well as long-wavelength lines of the oxygen Schumann–Runge $X^3\Sigma_g^- - B^3\Sigma_u^-$ (300–460) band [20].

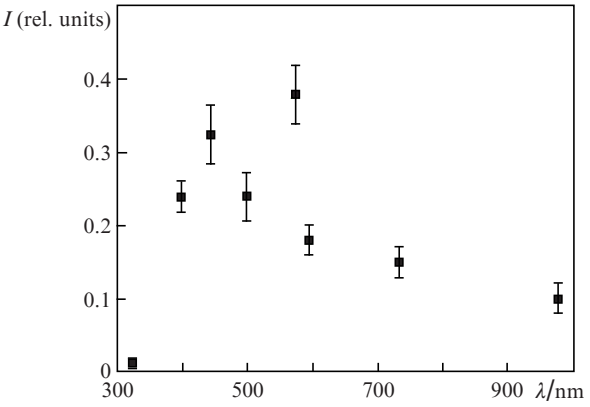


**Figure 3.** Intensity distribution of the glow region of the thermal track as a function of wavelength at a distance of 8 mm from the plasmoid; the antechamber pressure is 8 atm.

Further investigations of the glow of the thermal track were carried out with the monochromator adjusted to a wavelength of 555 nm at the slit width of 4 mm (which corresponds to the spectral width of 48 nm). Such a regime provides obtaining a sufficiently large signal from a moving cavern especially in measurements at large (greater than 20 mm) distances from the plasmoid.

The oscillogram of the FEM signal shown in Fig. 4 was obtained for the case where the optical system was adjusted to the point in a thermal track residing at a distance of 8 mm from the laser beam focusing point downward the flow. The pulse repetition rate was 50 kHz. The intensive light pulses, observed in the signal, followed the pulse repetition rate and corresponded to the exposure by a powerful light flash from the generated plasma. These pulses were used as a reference signal. Also the pulses of a lower power were detected, which arose at the instants depending on the distance between the focusing point of the detection optical system and the place of plasma formation (Fig. 4a). These light pulses refer to emission of the discrete high-temperature caverns of low density, which arise due to an optical breakdown under the action of high-power focused laser radiation and fly by the focusing point of the detection system. The delay of these pulses relative to the laser pulses and their shape depended on the distance from the point of plasmoid formation and on the velocity of the flow determined by the pressure in the antechamber (Fig. 4b).

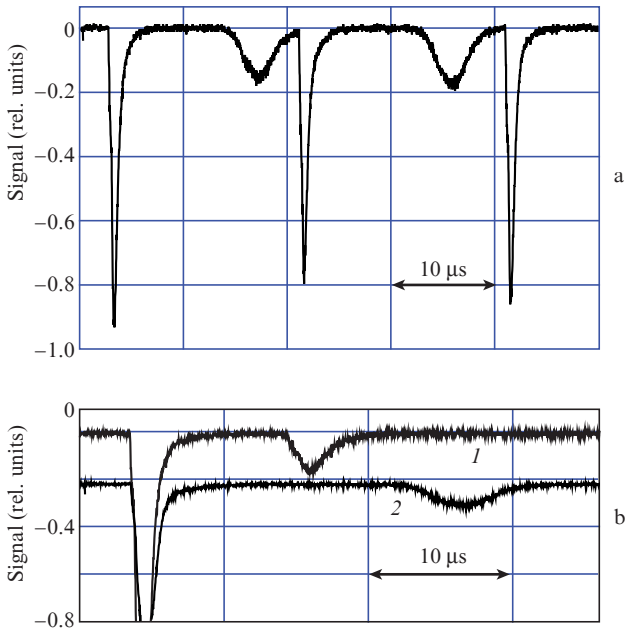


**Figure 4.** Oscillograms of glow pulses of the thermal track region at a distance of 8 mm from the plasmoid; the antechamber pressure is 8 (a), 10 (*1*; b) and 2 atm (*2*; b), the pulse repetition rate is 50 (a) and 30 kHz (b).

The time needed for the cavern to cover a distance of ~10 mm from the plasmoid at the characteristic flow velocity of 500 m s$^{-1}$ was ~20 μs, which corresponds to the time interval between the pulses at their repetition rate of 50 kHz. Hence, the pulse of the cavern glow will coincide with the glow of the plasmoid generated in a subsequent optical breakdown; at the distance from the plasmoid 15 mm it will be approximately in the middle of the interval between successive glow pulses of the plasmoid. In order to study the flow velocity (cavern motion) in a thermal track versus the distance from the plasmoid and air pressure, a lower frequency of pulses was used in the antechamber (7 kHz), which was determined by the modulator having a less number of cuts, but, the same velocity of rotation.

The results of glow detection at the three points in the thermal track separated from the plasmoid by distances of 8, 13, and 21 mm are shown in Fig. 5 for the pulse repetition rate of 7 kHz and the time interval between pulses 140 μs. The time needed for the cavern to pass from one point to the other was measured by positions of centres of cavern images. In this way, *RT*-diagram was obtained and the dependence of the flow velocity $V$ on the distance from the plasmoid was plotted (Fig. 6). At a 'zero point' the flow velocity was calculated taking into account the stationary supersonic flow at the pressure of 8 atm in the antechamber [9]. One can see from Fig. 6 that at a distance of 4 mm from the plasmoid the flow velocity increases to 650 μs$^{-1}$ and then it reduces to 360 μs$^{-1}$. From oscillograms (Fig. 5) and measured velocity values (Fig. 6) one can estimate the characteristic dimension of the cavern $d = V\tau$, where $\tau$ is the zero-level pulse duration. For distances of 8–13 mm we obtain the cavern dimension of ~4–5 mm.

From the cavern dimensions and average flow velocity one can find the critical pulse repetition rate $f_{crit} = V/d$ needed for caverns to unite into a solid track of a low-density hot jet. By using the characteristic parameters $d$ = 4–5 mm and $V$ = 500 m s$^{-1}$ we obtain a minimal frequency of 80–100 kHz.

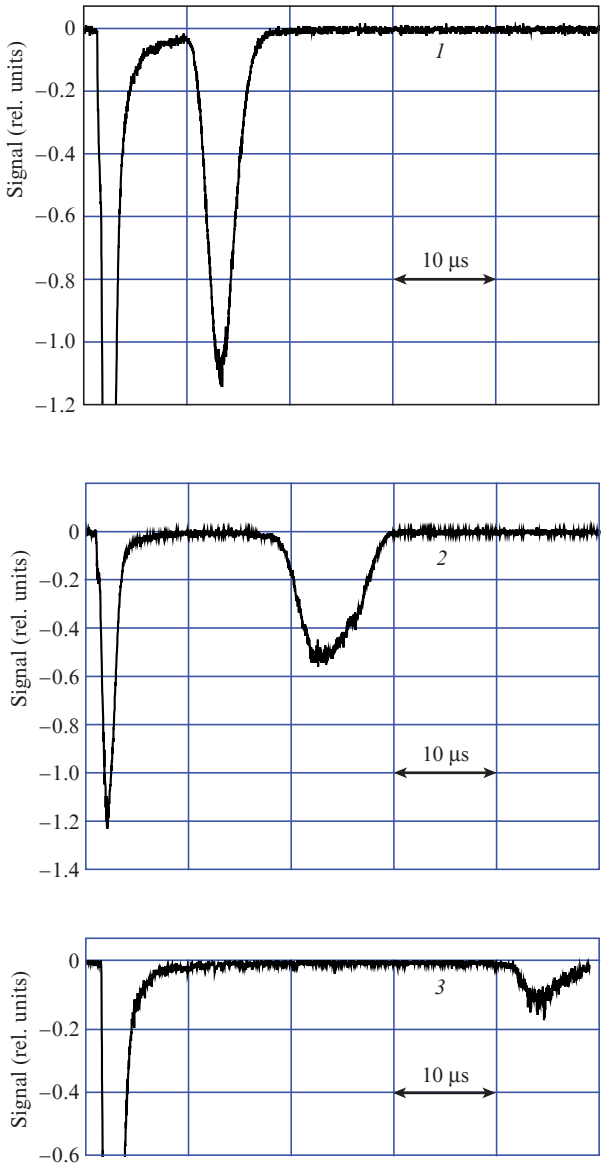


**Figure 5.** Oscillograms of glow pulses of the thermal track region at a distance of 8 (*1*), 13 (*2*) and 21 mm (*3*) from the plasmoid; the antechamber pressure is 8 atm.

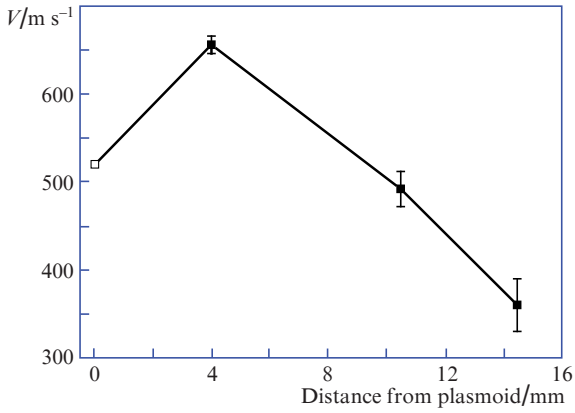


**Figure 6.** Flow velocity vs. distance from the plasmoid. The white square shows the calculated velocity.

In order to realise this regime, the laser system [9–11] was improved for obtaining the pulse repetition rate of the low-pressure $CO_2$ laser up to 120 kHz at the average power of up to 4 kW.

Oscillograms of glow pulses for the regions of the thermal track separated from the plasmoid by the distances of 8 and 13 mm are shown in Fig. 7 at the antechamber pressure of 8 atm and the pulse repetition rate of 120 kHz. These oscillograms are specific, as compared to those in Fig. 4, in that they have a constant component (if the corresponding oscilloscope input is open for the DC), i.e., they show a detected constant glow of the thermal track. This fact proves that at the frequency of 120 kHz the caverns unite into a light filament modulated at the frequency of laser pulses.

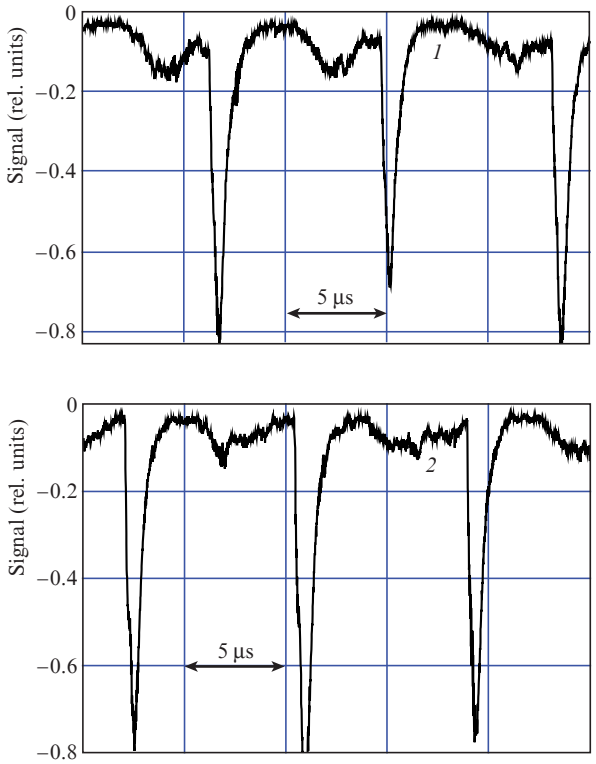


**Figure 7.** Oscillograms of glow pulses of the thermal track region at a distance of 8 (*1*) and 13 mm (*2*) from the plasmoid; the antechamber pressure is 8 atm and the pulse repetition rate is 120 kHz.

Oscillograms of all light signals observed in system operation are shown in Fig. 8. Oscillograms (*1*) and (*2*) correspond to incident laser radiation and radiation passed through the plasmoid, oscillogram (*3*) is responsible for the plasmoid light detected by a FK-22 vacuum photocell (see Fig. 1) with a high temporal resolution (~5 ns), and oscillogram (*4*) corresponds to the thermal track radiation detected by the FEM. One can see that the signal from the FEM flattens high-frequency details and well describes the main shape of the plasma glow pulse. Power measurements of incident and passed laser radiation made it possible to determine the absorption coefficient of radiation in the plasmoid by using a method similar to that in [9–11]. The absorption coefficient was found to be 70%, i.e, close to the values measured earlier at a lower frequency. It was shown in [11] that reflection and refraction are negligible in the process of plasma formation.

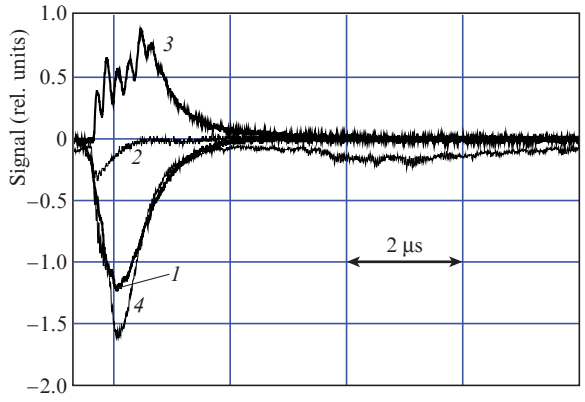


**Figure 8.** Oscillograms of optical signals: incident (*1*) and passed (*2*) laser radiation, light from the plasmoid (*3*) and thermal track emission (*4*).

## 4. Discussion

Generation of a quasi-continuous high-enthalpy thermal track of low density is of great importance for efficient controlling a supersonic air flow because such a track has some advantages as compared to a discrete repetitively pulsed track. In particular, it opens the possibility to more efficiently absorb the energy of high-frequency generators, control the structure of shock waves and the process of controlled burning in a supersonic flow and so on. Consider the conditions for generation of a quasi-continuous low-density thermal track in more details.

First of all it should be noted that creation of the plasma cloud is accompanied by formation of a shock wave in ambient gas. This wave overtakes the cavern generated earlier and affects it. Our measurements lead to a conclusion that such an interaction does not destroy the thermal track. At a low repetition rate of pulses the shock wave noticeably weakens and no action to the cavern glow is observed (see Fig. 4). At a high pulse repetition rate (see Fig. 6) when caverns merge, the glow intensity oscillates, which can be interpreted as deformation of the hot gas cloud. However, in this case, separate bunches of the glowing hot gas are definitely distinguished, i.e., no fast destruction of clouds is observed.

Formation of a single plasmoid is well described by the point explosion theory with a back pressure taken into account, which is thoroughly described in [16, 18]. The radius $R_0$ of a spherical cavern at the stage of its quasi-stationary cooling can be estimated, similarly to [17], by using the formula

$$R_0 = \left[\frac{3AQ}{4\pi(W_\tau + W_\infty)}\right]^{1/3},$$

where $Q$ is the energy of a single pulse; $A$ is the absorption coefficient of laser radiation in plasma; $W_\tau \approx 0.5$ J cm$^{-3}$ is the excess of heat concentration in the cavern at the stage of its isobaric cooling [18, 19, 21]; and $W_\infty$ is enthalpy of undisturbed gas. In our case, at the average power of laser radiation 4 kW, pulse repetition rate of 120 kHz, and the absorption coefficient $A = 0.7$ we obtain $R_0 \approx 3.3$ mm, which is close to the experimental value.

By using the relationships $f_{crit} = V/d$, $d = 2R_0 = BQ^{1/3}$ and $P_{crit} = Q f_{crit}$ we find the relation between the critical power of laser radiation $P_{crit}$, pulse repetition rate $f_{crit}$, and velocity of the supersonic flow $V$ at which caverns unite: $P_{crit} \approx V^3 \times (B^3 f_{crit}^2)^{-1}$. Here we employed the fact $B$ = const. Thus, an increase in the average power cannot noticeably raise the flow velocity. Cavern merging, for example, at a double velocity (to 1000 m s$^{-1}$) would require the eight times greater power. It is more reasonable to increase the pulse repetition rate. In this case, the parameters of a single pulse (in particular, the peak power) should provide efficient formation of plasma [9]. This stimulates investigations of energy characteristics of $CO_2$ lasers possessing high pulse repetition rates (100 kHz and greater) and relaxation processes in the active media of such lasers.

## 5. Conclusions

From the experimental results discussed above one may come to the following conclusions.

1. For the first time, stable discrete objects, namely, low-density caverns moving with a flow are detected in the OPD by the optical method.

2. Velocities are measured of the thermal track arising in a supersonic flow under the action of the OPD.

3. It was established that at pulse repetition rates of 90–120 kHz, low-density caverns unite into a single plasma jet.

## References

1. Ellinwood J.W., Mirels H. *Appl. Opt*., **14**, 2238 (1975).
2. Akhmanov S.A., Rudenko O.V., Fedorchenko A.T. *Pis'ma Zh. Tekhn. Fiz*., **5**, 934 (1979).
3. Bagayev S.N., Grachev G.N., Ponomarenko A.G., Smirnov A.L., Demin V.N., Okotrub A.V., Baklanov A.M., Onischuk A.A. *Proc. SPIE Int. Soc. Opt. Eng*., **6732**, 6732062 (2007).
4. Zudov V.N., Grachev G.N., Krainev V.L., Smirnov A.L., Tret'yakov P.K., Tupikin A.V. *Fizika Goreniya i Vzryva*, **49** (2), 144 (2013) [*Combustion, Explosion, and Shock Waves*, **49** (2), 254 (2013)].
5. Tretyakov P.K., Grachev G.N., Ivanchenko A.I., Kraynev V.L., Ponomarenko A.G., Tischenko V.N. *Dokl. Ross. Akad. Nauk*, **336**, 466 (1994).
6. Bagayev S.N., Grachev G.N., Ponomarenko A.G., Smirnov A.L., Demin V.N., Okotrub A.V., Barlanov A.M., Onishchuk A.A. *Nauka i nanotekhnologii (Science and Nanotechnologies)* (Novosibirsk: Izd. SO RAN, 2007) p.123.
7. Tischenko V.N., Grachev G.N., Pavlov A.A., Smirnov A.L., Pavlov Al.A., Golubev M.P. *Kvantovaya Elektron*., **38**, 82 (2008) [*Quantum Electron*., **38**, 82 (2008)].
8. Tischenko V.N., Apollonov V.V., Grachev G.N., Gulidov A.I., Zapryagaev V.I., Men'shikov Ya.G., Smirnov A.L., Sobolev A.V. *Kvantovaya Elektron*., **34**, 941 (2004) [*Quantum Electron*., **34**, 941 (2004)].
9. Malov A.N., Orishich A.M., Shulyat'ev V.B. *Kvantovaya Electron*., **41**, 1027 (2011) [*Quantum Electron*., **41**, 1027 (2011)].
10. Malov A.N., Orishich A.M. *Pis'ma Zh. Tekhn. Fiz*., **38**, 32 (2012).
11. Malov A.N., Orishich A.M. *Kvantovaya Elektron*., **42**, 843 (2012) [*Quantum Electron*., **42**, 843 (2012)].
12. Garanin A.F., Tret'yakov P.K., Chirkashenko V.F., Yudintsev Yu.N. *Izv. Ross. Akad. Nauk, Ser. Mekh. Zhidk. Gaza*, (5), 186 (2001).
13. Raizer Yu.P. *Lazernaya iskra i rasprostraneniye razryadov* (Laser Spark and Discharge Propagation) (Moscow: Nauka, 1980).
14. Borzov Yu.V., Mikhailov V.M., Rybka I.V., Savishchenko N.P., Yur'ev A.S. *Inzh.-Fiz. Zh*., **66**, 515 (1994).
15. Bufetov I.A., Prokhorov A.M., Fedorov V.B., Fomin V.K. *Dokl. Akad. Nauk SSSR*, **261**, 586 (1981).
16. Zvorykin V.D., Ionin A.A., Levchenko A.O., Mesyats G.A., et al. *Kvantovaya Elektron*., **43**, 339 (2013) [*Quantum Electron*., **43**, 339 (2013)].
17. Kabanov S.N., Maslova L.I., Terekhova T.A., Trukhin V.A., Yurov V.T. *Zh. Tekhn. Fiz*., **60**, 37 (1990).

18. Kononenko V.V., Kononenko T.V., Pashinin V.M., Konov V.I. *Kvantovaya Elektron*., **43**, 356 (2013) [*Quantum Electron*., **43**, 356 (2013)].
19. Korobeinikov V.P. In: *Trudy ordena Lenina Matematicheskogo instituta imeni V.A. Steklova* (Proceedings of V.A. Steklov Institute of Mathematics) (Moscow: Nauka, 1973) p. 268.
20. Avilova I.V., Biberman L.M., Vorob'yov V.S., et al. *Opticheskie svoistva goryachego vozdukha* (Optical properties of Hot Air) (Moscow: Nauka, 1962) p. 320.
21. Predvoditelev A.S., Stupochenko E.V., Pleshakov A.S., et al. *Tablitsy termodinamicheskikh funktsii vozdukha* (Tables of Thermodynamic Functions of Air) (Moscow: izd. Vych. Tsentra AN SSSR, 1970) p. 320.